Am J Cancer Res 2025;15(5):2413-2426
www.ajcr.us /ISSN:2156-6976/ajcr0164534

Original Article

The complex interplay of TROP2 and PD-L1 in immune regulation and drug resistance in lung cancer

Chih-Jen Yang[1,5], Cheng-Hao Chuang[1,6], Yin-Wen Chen[2], Ching-Tang Huang[7], Pei-Hui Wang[7], Yen-Yi Zhen[8], Saud Ali Shah[2], Misbah Sehar[2], Po-Kai Chuang[2,3,4]

[1]Division of Pulmonary and Critical Care Medicine, Department of Internal Medicine, Kaohsiung Medical University Hospital, Kaohsiung Medical University, Kaohsiung, Taiwan; [2]Institute of Biomedical Sciences, College of Medicine, National Sun Yat-sen University, Kaohsiung, Taiwan; [3]Department of Biological Sciences, National University of Kaohsiung, Kaohsiung, Taiwan; [4]Kaohsiung Medical University, Kaohsiung, Taiwan; [5]School of Post-Baccalaureate Medicine, College of Medicine, Kaohsiung Medical University, Kaohsiung, Taiwan; [6]Graduate Institute of Medicine, College of Medicine, Kaohsiung Medical University, Kaohsiung, Taiwan; [7]Department of Internal Medicine, KaohsiungMedical University Hospital, Kaohsiung Medical University, Kaohsiung, Taiwan; [8]Division of Nephrology, Department of Internal Medicine, Kaohsiung Medical University Hospital, Kaohsiung Medical University, Kaohsiung, Taiwan

Received March 14, 2025; Accepted May 13, 2025; Epub May 25, 2025; Published May 30, 2025

Abstract: The complex interplay of TROP2 and PD-L1 in lung adenocarcinoma (LUAD) influences drug resistance and immunotherapy efficacy remains incompletely understood yet. In this study, we investigated the relationship between TACSTD2 (encoding TROP2) and PD-L1 expression through transcriptome analysis, immunohistochemistry, and single-cell RNA sequencing in lung cancer cell lines, tumor tissues, and immune cells, focusing on PC9 parental and drug-resistant variants. TACSTD2 expression strongly correlated with poor clinical outcomes, particularly in immunotherapy-treated patients (HR 1.71 for OS, 2.95 for PFS). Our transcriptome analysis revealed distinct resistance mechanisms involving MAPK signaling and immune receptor regulation pathways. Immunohistochemistry demonstrated significantly elevated TROP2 expression in tumor tissues compared to normal samples, with notably higher levels in PD-L1 positive specimens. We observed significant negative correlations between TACSTD2 expression and $CD8^+$ T cell infiltration (Rho = -0.11, P = 1.44e-02), alongside positive correlations with cancer-associated fibroblasts (Rho = 0.094, P = 3.68e-02). Single-cell RNA sequencing identified two distinct cancer subtypes with differential TACSTD2 expression, while gene ontology analysis highlighted enrichment in cell adhesion and immune interaction pathways. These findings provide novel insights into the molecular mechanisms underlying TROP2 and PD-L1 interactions in LUAD, offering potential new diagnostic markers and therapeutic strategies through improved understanding of tumor microenvironment dynamics and resistance mechanisms.

Keywords: TROP2, PD-L1, lung adenocarcinoma, drug resistance, immunotherapy

Introduction

Lung cancer remains the leading cause of cancer-related mortality worldwide, with drug resistance posing a critical challenge [1]. Despite advances in immunotherapy and targeted approaches, response rates to immune checkpoint inhibitors in NSCLC remain limited at 20-30% [2]. Recent studies have revealed intricate signaling cascades linking TROP2 and PD-L1 expression [3], with the PI3K/AKT/mTOR and MAPK pathways serving as critical mediators [4]. TROP2 activation influences PD-L1 expression through both transcriptional and post-translational modifications, further complicated by feedback loops involving inflammatory cytokines [5]. TROP2 overexpression correlates with poor prognosis and increased tumor aggressiveness [6], while TROP2-targeted antibody-drug conjugates, such as Datopotamab Deruxtecan, have demonstrated promising clinical efficacy [7].

TROP2 signaling also influences T cell activation, exhaustion marker expression, memory T cell formation, and cytokine production [8]. Furthermore, it affects myeloid cell function by regulating suppressor cell recruitment and

macrophage polarization, thereby contributing to the immunosuppressive tumor microenvironment [9]. PD-L1 expression dynamics during treatment exhibit remarkable complexity, with emerging evidence suggesting significant plasticity in response to various therapeutic interventions [10]. Novel regulatory mechanisms of PD-L1 expression include post-translational modifications affecting protein stability, epigenetic regulation, stress-induced adaptive responses, and the effects of metabolic reprogramming [11].

The interplay between TROP2 and PD-L1 signaling pathways represents a critical area for therapeutic intervention, as combined targeting of both pathways may enhance treatment efficacy [12]. Emerging evidence suggests that acquired resistance to both TROP2-targeted therapies and immune checkpoint inhibitors involves complex adaptive mechanisms [13], including alterations in epithelial-mesenchymal transition (EMT) programs, metabolic reprogramming, and modifications in cellular stress response pathways. Multi-omics analyses have identified specific resistance signatures characterized by concurrent changes in both TROP2 and PD-L1 signaling networks [14].

Phase I/II clinical trials investigating the combination of TROP2-targeted antibody-drug conjugates with PD-1/PD-L1 inhibitors have shown encouraging preliminary results [15]. Novel therapeutic approaches under development include bi-specific antibodies targeting both TROP2 and PD-L1, engineered T cells directed against TROP2-expressing tumors, and innovative delivery systems for combined targeted therapy [16]. Preclinical studies demonstrate superior efficacy of these strategies compared to conventional monotherapies. Moreover, the integration of multi-modal biomarker data has led to the development of predictive algorithms using machine learning techniques to analyze complex patterns and predict optimal treatment strategies for individual patients [3].

This study investigates the molecular crosstalk between TROP2 and PD-L1 in NSCLC, focusing on expression patterns, regulatory relationships, and their roles in immune evasion and drug resistance. We examine how TROP2 influences the PI3K/AKT/mTOR and MAPK pathways, impacts immune cell function, and contributes to resistance mechanisms including EMT and metabolic reprogramming. Understanding these signaling networks represents a critical step toward developing more effective cancer therapies. By identifying key molecular mediators, validating regulatory networks through functional studies, and evaluating clinical relevance in drug-resistant lung cancer, we aim to advance therapeutic strategies. Future research should explore temporal dynamics during treatment, develop adaptive therapeutic approaches based on real-time monitoring, and integrate molecular and clinical data to better predict and overcome drug resistance in lung cancer.

Materials and methods

Cell culture and sample preparation

PC9 (parental), PC9-IR (Gefitinib resistant, 10 μM), and PC9-ER (Erlotinib resistant, 10 μM) cells were cultured in RPMI-1640 medium with 10% fetal bovine serum and 1% penicillin/streptomycin at 37°C with 5% CO_2, and harvested at 80% confluence for RNA extraction.

Expression and survival analysis

TACSTD2 (TROP2) expression in lung adenocarcinoma (LUAD) was analyzed using Kaplan-Meier Plotter (https://kmplot.com/analysis/index.php?p=service&cancer=lung or https://kmplot.com/analysis/index.php?p=service&cancer=immunotherapy) and GEPIA 2 (http://gepia2.cancer-pku.cn/#analysis) platforms to evaluate correlations with survival rates and immunotherapy efficiency. TCGA samples were compared with normal samples for pan-cancer analysis and LUAD-specific expression patterns. Overall survival (OS) and progression-free survival (PFS) analyses were performed in relation to TACSTD2 expression levels.

Western blot analysis

Parental PC9 cells and resistant variants (PC9-IR with 10 μM Gefitinib and PC9-ER with 10 μM Erlotinib) were harvested at 80% confluence and lysed in RIPA buffer with protease inhibitor cocktail (Roche) and phosphatase inhibitors (Sigma-Aldrich). Protein concentration was determined using BCA Protein Assay Kit (Pierce). Equal amounts (30 μg) were separated by 10% SDS-PAGE, transferred to PVDF membranes (Millipore), blocked with 5% non-

fat milk, and incubated with primary antibodies against TROP2 (abcam), PD-L1 (abconal), and β-actin (abclonal). After washing, membranes were incubated with HRP-conjugated secondary antibodies (Jackson ImmunoResearch) and visualized using ECL reagent (Pierce) on Chemiscope S6 Imaging System.

RNA sequencing and library preparation

Total RNA was extracted using TRIzol reagent (Invitrogen) following manufacturer's protocol. RNA quality was assessed using Agilent 2100 Bioanalyzer (all samples RIN > 8.0). RNA-seq libraries were prepared using Illumina TruSeq Stranded mRNA Library Prep Kit and sequenced as 150 bp paired-end reads on Illumina NovaSeq 6000 platform.

Raw sequencing reads were quality-checked using FastQC (v0.11.9) and trimmed with Trimmomatic (v0.39). Clean reads were aligned to human reference genome (GRCh38) using STAR aligner (v2.7.3a). Gene expression was quantified using HTSeq-count (v0.13.5) and differential expression analysis performed with DESeq2 (v1.30.1), with adjusted p-value < 0.05 and |log2FoldChange| > 1 considered significant.

Pathway and gene set enrichment analysis

KEGG pathway and Gene Ontology analyses were performed using clusterProfiler (v3.18.1). Gene Set Enrichment Analysis (GSEA) was conducted using GSEA software (v4.1.0) with MSigDB hallmark gene sets, with enrichment significance determined by FDR < 0.25 and nominal p-value < 0.05.

Immunohistochemical analyses

A lung cancer tissue microarray (LC401a from US Biomax Inc.) containing 40 cases of lung adenocarcinoma was utilized alongside a PD-L1 tested non-small cell lung carcinoma tissue microarray with 20 cases each of PD-L1 negative and positive samples. Following deparaffinization, rehydration, peroxidase blocking, and citrate buffer (pH 6.0) antigen retrieval, sections were incubated with anti-TROP2 primary antibody (abcam) overnight at 4°C, then with HRP-conjugated secondary antibody. Visualization used DAB chromogen with hematoxylin counterstaining. Sections were examined using a Nikon ECLIPSE-Ci microscope and analyzed with Image J software to assess TROP2 expression patterns in tumor versus normal tissues.

Data collection and processing

Single-cell RNA sequencing (scRNA-seq) data was obtained from the Gene Expression Omnibus (GEO) database using dataset GSE117570, which comprises 4 non-small cell lung cancer tumor samples and 4 matched paracancerous tissue samples, providing comprehensive transcriptomic profiles at single-cell resolution for characterizing cellular heterogeneity within the tumor microenvironment.

Single-cell RNA-seq data processing

Raw gene expression matrices were processed using Seurat package (version 4.4.2) in R. Quality control filtered cells based on: minimum 100 gene features per cell, minimum 10 cells per gene, maximum 5,000 gene features per cell, maximum 20% mitochondrial gene percentage, and minimum 10 UMI count per cell. Data was normalized using "LogNormalize" method, multiplied by a scale factor of 10,000, and log-transformed. The top 2,000 highly variable genes were identified using FindVariableFeatures function with "vst" method. Batch effects were mitigated through integration using FindIntegrationAnchors and IntegrateData functions. Dimensionality reduction was performed using PCA, with the first 50 principal components used for UMAP visualization and graph-based clustering.

Cell cluster analysis

We performed unsupervised clustering that was performed using FindNeighbors and FindClusters functions in Seurat, utilizing the first 50 principal components with the Louvain algorithm at a resolution of 1.0, resulting in 20 distinct cell clusters visualized by UMAP. Cell clusters were identified through differential expression analysis using the FindConservedMarkers function. Cancer and T cell subpopulations were identified using literature-defined markers: Cancer I (SOX2 cancer cells) by EPCAM, KRT17, S100A2, SFN, PTHLH, and PERP; Helper CD4 T cells by KLRB1; Cancer II (alveolar cells) by SFTPC, SCGB3A1, SFTPB, WFDC2, and MUC1; CD8 T cells by CD8A/B;

naïve T cells by CCR7 and TCF7; and NK cells by KLRF1 and NKG7. Cell type proportions were compared between tumor and paracancerous samples to evaluate tumor microenvironment composition changes.

Identification of cell marker gene-functional enrichment analysis

Cell marker genes between cancer subpopulations were identified through differential expression analysis using Seurat's FindMarkers function with Wilcoxon rank-sum test (min.pct = 0.25, logfc.threshold = 0.25). Gene ontology (GO) pathway enrichment analysis was performed using clusterProfiler package (version 4.14.4) to identify characteristic biological processes between cancer subpopulations. Gene symbols were converted to Entrez IDs, and genes with adjusted *p*-value < 0.05 and |log2FC| > 0.25 were analyzed, applying Benjamini-Hochberg method for multiple testing corrections.

Function enrichment and ssGSEA analysis

All statistical analyses were performed in R (version 4.4.2). Statistical significance was defined as adjusted *p*-value < 0.05. Visualization of results was performed using ggplot2 and ggpubr packages.

Statistical analysis

The scRNA-seq dataset analyzed in this study is publicly available in the Gene Expression Omnibus (GEO) under the accession number GSE117570. The R scripts used for data processing and analysis are provided in the supplementary data.

Availability of data and materials

The datasets used and/or analyzed in the present study are available from the corresponding author on reasonable request.

Results

TACSTD2 gene (encode TROP2 protein) expression correlates with poor immunotherapy response and reduced survival in lung adenocarcinoma

Our comprehensive analysis reveals that TACSTD2 (Tumor-Associated Calcium Signal Transducer 2) expression significantly impacts patient outcomes and immunotherapy response in lung adenocarcinoma (LUAD). Initial examination of TACSTD2 expression patterns demonstrated notably elevated levels in LUAD tumor tissues compared to adjacent normal tissues (n = 483 vs. n = 347, P < 0.05), suggesting a potential role in tumor development (**Figure 1A**). In survival analyses of the general LUAD cohort, patients with high TACSTD2 expression exhibited significantly poorer overall survival (OS) compared to those with low expression (HR = 1.48, 95% CI: 1.25-1.76, P = 5.4e-06). This trend was similarly reflected in progression-free survival (PFS) analyses (HR = 1.26, 95% CI: 1.12-1.42, P = 0.00018), indicating the potential of TACSTD2 as a prognostic marker (**Figure 1B** and **1C**).

The impact of TACSTD2 expression was even more pronounced in immunotherapy-treated patients, where high expression correlated with worse overall survival (HR = 1.71, 95% CI: 1.27-2.29, P = 0.00031) and dramatically reduced progression-free survival (HR = 2.95, 95% CI: 2.14-4.07, P = 4.7e-12) (**Figure 1D**, **1E**). Protein expression analysis revealed complex interactions among TACSTD2, PD-L1, and TROP2 across different cell lines. Western blot analysis showed varying expression patterns in PC9, PC9-IR (Gefitinib-resistant), and PC9-ER (Erlotinib-resistant) cells, suggesting potential regulatory relationships (**Figure 1F**). The strong association between high TACSTD2 expression and poor immunotherapy outcomes highlights its potential utility in patient stratification. Further investigation into the underlying molecular mechanisms may reveal new therapeutic targets for improving immunotherapy efficacy in LUAD patients.

Transcriptional landscape analysis reveals distinct molecular signatures in drug-resistant lung cancer cells

To elucidate the molecular mechanisms underlying drug resistance in lung cancer, we performed a comprehensive transcriptome analysis comparing PC9-IR and PC9-ER cells with parental PC9 cells. This analysis revealed distinct gene signatures, identifying 1360 differentially expressed genes in PC9-IR cells and 187 in PC9-ER cells. Notably, 275 genes were commonly dysregulated in both resistant popu-

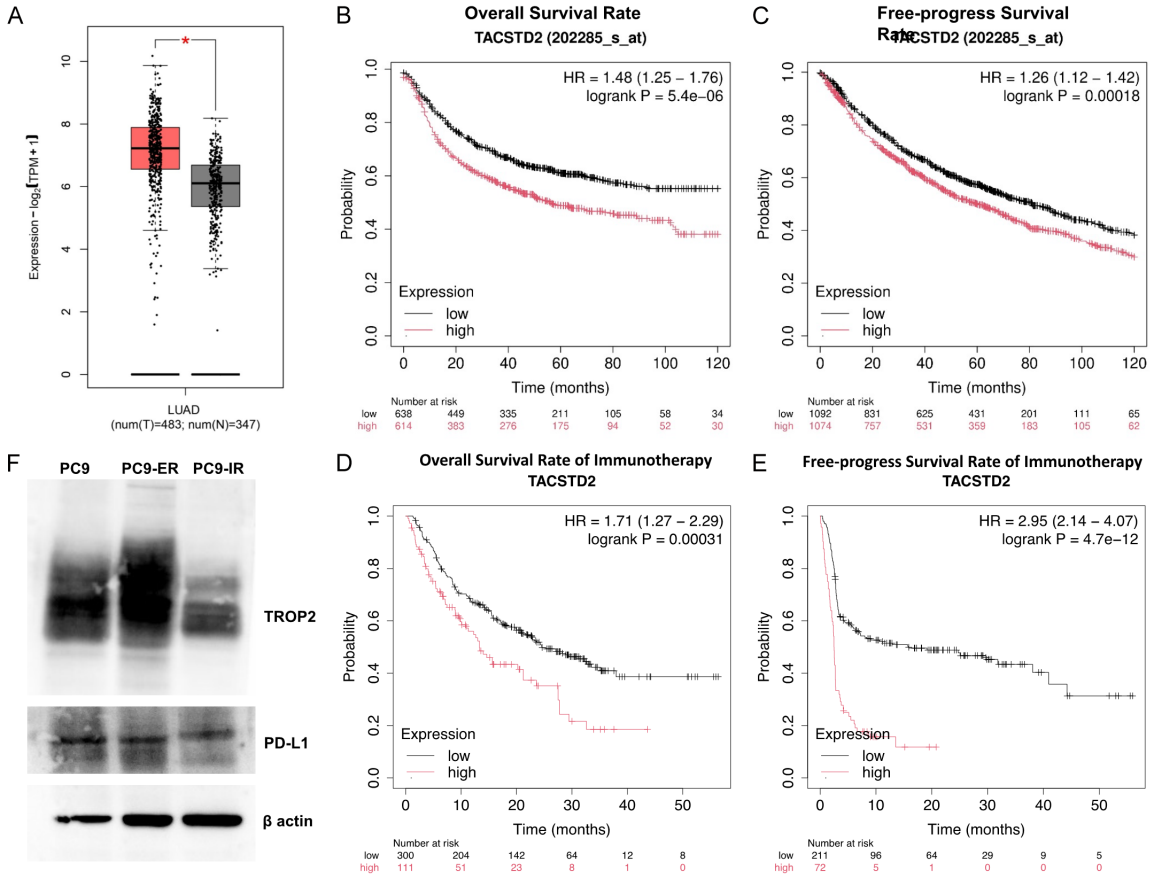

Figure 1. TACSTD2 expression impacts survival outcomes and correlates with treatment resistance. (A) Box plot demonstrating significantly higher TACSTD2 expression in LUAD tumor samples (n = 483) compared to normal tissues (n = 347) (P < 0.05). (B, C) Kaplan-Meier analysis in general LUAD cohort shows patients with high TACSTD2 expression exhibit poorer overall survival (HR = 1.48, 95% CI: 1.25-1.76, P = 5.4e-06) (B) and progression-free survival (HR = 1.26, 95% CI: 1.12-1.42, P = 0.00018) (C) over 120 months. (D, E) This survival difference becomes more pronounced in immunotherapy-treated patients, with high TACSTD2 expression associated with markedly worse overall survival (HR = 1.71, 95% CI: 1.27-2.29, P = 0.00031) (D) and dramatically reduced progression-free survival (HR = 2.95, 95% CI: 2.14-4.07, P = 4.7e-12) (E) over 50 months. (F) Western blot analysis reveals differential expression patterns of TROP2 and PD-L1 across parental (PC9) and resistant (PC9-IR, PC9-ER) cell lines, with PC9-ER showing notably increased TROP2 expression while PC9-IR shows reduced expression compared to parental cells, suggesting resistance-specific regulation of these proteins.

lations, suggesting a core resistance signature (**Figure 2A**). Hierarchical clustering analysis of the differentially expressed genes revealed distinct expression patterns across the three cell populations, highlighting the dynamic transcriptional reprogramming that occurs during resistance development (**Figure 2B**). MA and volcano plots visualized the expression changes in ER versus PC9 (**Figure 2C**) and IR versus PC9 (**Figure 2D**) comparisons. Key differentially expressed genes in ER cells included upregulated SERPINE1, MAGEA4, and TPM1, while IR cells showed significant upregulation of SALL2, SERPINB5, and ALDH1A3.

Pathway analysis was conducted to further elucidate the biological mechanisms underlying EGFR-TKI resistance, revealing distinct functional signatures between the resistance models. Gene Set Enrichment Analysis in erlotinib-resistant cells demonstrated significant enrichment of the MAPK cascade (**Figure 2E**), with additional Gene Ontology (GO) analysis identifying enriched pathways including regulation of cell adhesion, the ERK1/ERK2 cascade, and extracellular matrix organization (**Figure 2F**). The transcriptome analysis revealed significant enrichment of the MAPK cascade in erlotinib-resistant cells, suggesting that this pathway

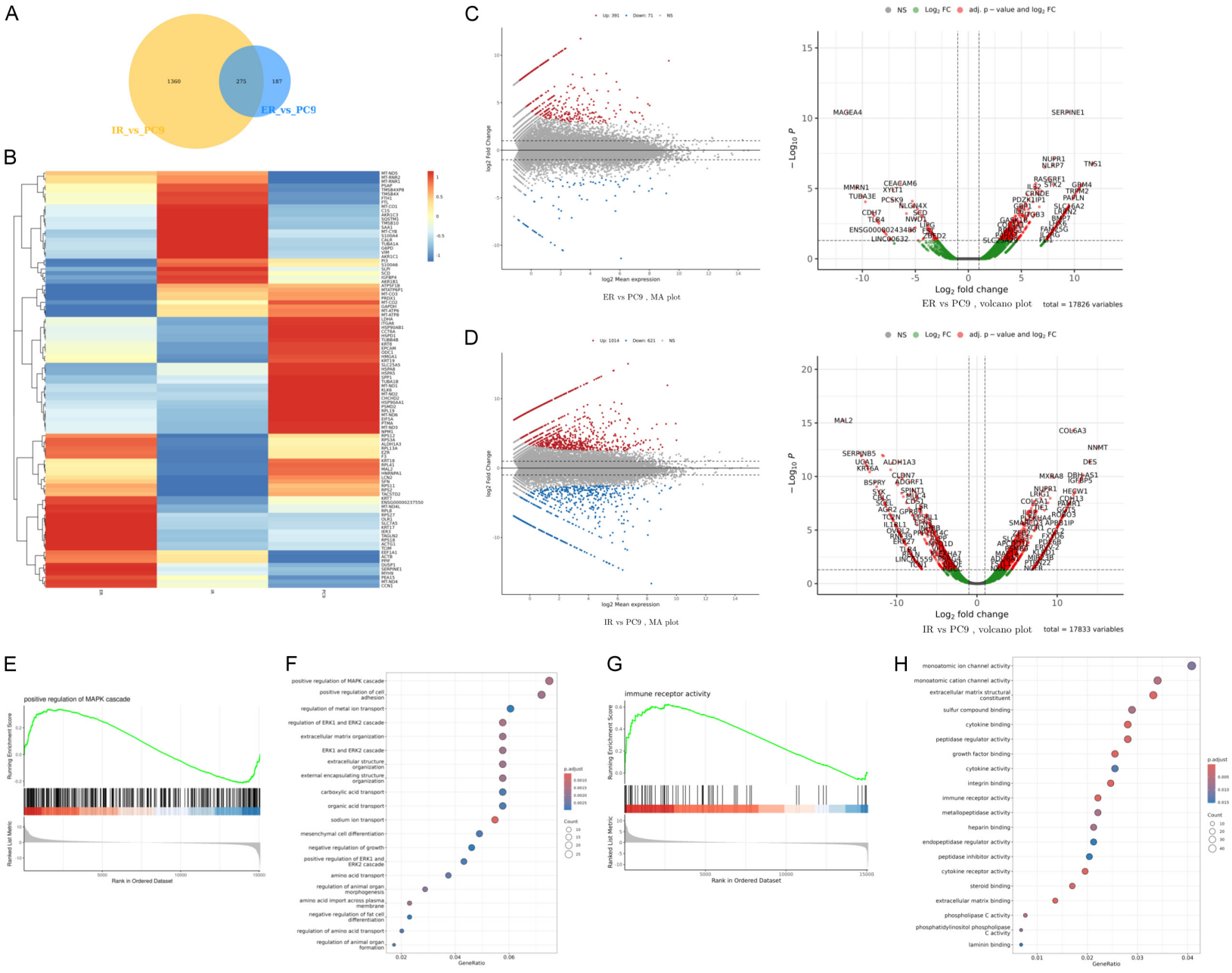
A
1360
275
187
IR_vs_PC9
ER_vs_PC9
B
C
ER vs PC9 , MA plot
ER vs PC9 , volcano plot
total = 17826 variables
D
IR vs PC9 , MA plot
IR vs PC9 , volcano plot
total = 17833 variables
E
positive regulation of MAPK cascade
F
G
immune receptor activity
H

Figure 2. Differential gene expression and pathway analysis in EGFR-TKI resistant lung cancer cell lines. (A) Venn diagram showing the overlap of differentially expressed genes between IR vs PC9 (yellow circle, 1340 unique genes) and ER vs PC9 (blue circle, 187 unique genes) comparisons, with 275 shared genes between both conditions. (B) Hierarchical clustering heatmap of the top 100 most variable genes across three experimental conditions (PC9, IR, and ER), with expression patterns clearly separating resistant from parental cells. (C) MA plot (left) and Volcano plot (right) of ER vs PC9 comparison, showing 621 upregulated and 465 downregulated genes (adjusted *p*-value < 0.05, |log2FC| > 1), with key upregulated genes including SERPINE1, MAGEA4, and TPM1. (D) MA plot and Volcano plot of IR vs PC9 comparison, revealing more extensive transcriptional changes with 834 upregulated and 45 downregulated genes, including significantly upregulated SALL2, SERPINB5, and ALDH1A3. (E-H) Pathway enrichment analysis showing distinct biological mechanisms in each resistance model: ER cells demonstrate significant enrichment of MAPK cascade regulation (E) along with cell adhesion, ERK/RAS signaling, and extracellular matrix organization (F), while IR cells show prominent enrichment of immune receptor activity (G), transmembrane receptor function, cytokine activity, and matrix binding (H). This analysis reveals MAPK signaling as predominant in erlotinib resistance and immune-related pathways in gefitinib resistance.

represents a key target for overcoming resistance. The notable enrichment of the ERK1/ERK2 cascade specifically indicates that MEK1/2 inhibitors (such as trametinib or cobimetinib) could be particularly effective in this patient population. Therefore, we propose that combining TROP2-targeted therapy (such as datopotamab deruxtecan) with MAPK inhibitors may provide synergistic effects. In contrast, gefitinib-resistant cells (IR) showed prominent enrichment of immune receptor activity (**Figure 2G**), along with transmembrane receptor functions, cytokine activity, and extracellular matrix binding (**Figure 2H**). These findings highlight distinct resistance mechanisms, with MAPK signaling predominant in erlotinib resistance and immune-related pathways in gefitinib resistance (PC9-IR), providing insights for the development of targeted therapeutic strategies to overcome resistance in lung adenocarcinoma.

TROP2 expression demonstrates strong correlation with PD-L1 status and is significantly elevated in lung adenocarcinoma

To investigate the relationship between TROP2 and PD-L1 expression in lung adenocarcinoma (LUAD), we performed a comprehensive immunohistochemical analysis of tumor tissue samples. TROP2 expression patterns were evaluated in PD-L1 null (n = 20) and PD-L1 positive (n = 20) LUAD specimens using immunohistochemistry. PD-L1 null samples (**Figure 3A-D**) predominantly exhibited weak to moderate TROP2 staining, whereas PD-L1 positive samples (**Figure 3E-H**) showed stronger and more widespread expression. Quantitative analysis confirmed higher TROP2 expression in PD-L1 positive samples (**Figure 3I**). This strong association suggests a potential regulatory relationship between TROP2 and PD-L1 expression in LUAD. Furthermore, comparative analysis between LUAD (n = 20) and normal tissue samples (n = 20) revealed significantly elevated TROP2 expression (log_2 TPM) in tumor tissues (Wilcoxon test statistic = 21600, P = 1.36e-07; **Figure 3J**). These findings indicate that TROP2 expression is significantly elevated in LUAD and positively associated with PD-L1 status, suggesting its potential utility as both a diagnostic marker and a predictor of PD-L1 expression, with implications for immune checkpoint regulation and therapeutic strategies.

TACSTD2 expression associates with distinct immune cell infiltration patterns and defines two major cancer subtypes in lung adenocarcinoma

To investigate the relationship between TACSTD2 expression and the tumor immune microenvironment in lung adenocarcinoma (LUAD), we analyzed its correlation with various immune cell populations. Our analysis revealed that TACSTD2 expression was negatively correlated with $CD8^+$ T cells (Rho = -0.11, P = 1.44×10^{-2}), particularly naive $CD8^+$ T cells (Rho = -0.135, P = 2.66×10^{-3}) and $CD4^+$ Th1 cells (Rho = -0.12, P = 7.84×10^{-3}), while showing a positive correlation with $CD4^+$ effector memory T cells (Rho = 0.092, P = 4.18×10^{-2}). A positive correlation was also observed between TACSTD2 expression and cancer-associated fibroblasts (CAFs) (Rho = 0.094, P = 3.68×10^{-2}), whereas no significant correlations were found with macrophage infiltration or tumor purity (**Figure 4A-I**).

Notably, the negative correlation between TACSTD2 expression and $CD8^+$ T cell infiltration (Rho = -0.11, P = 1.44×10^{-2}) provides important insights into the immunosuppressive

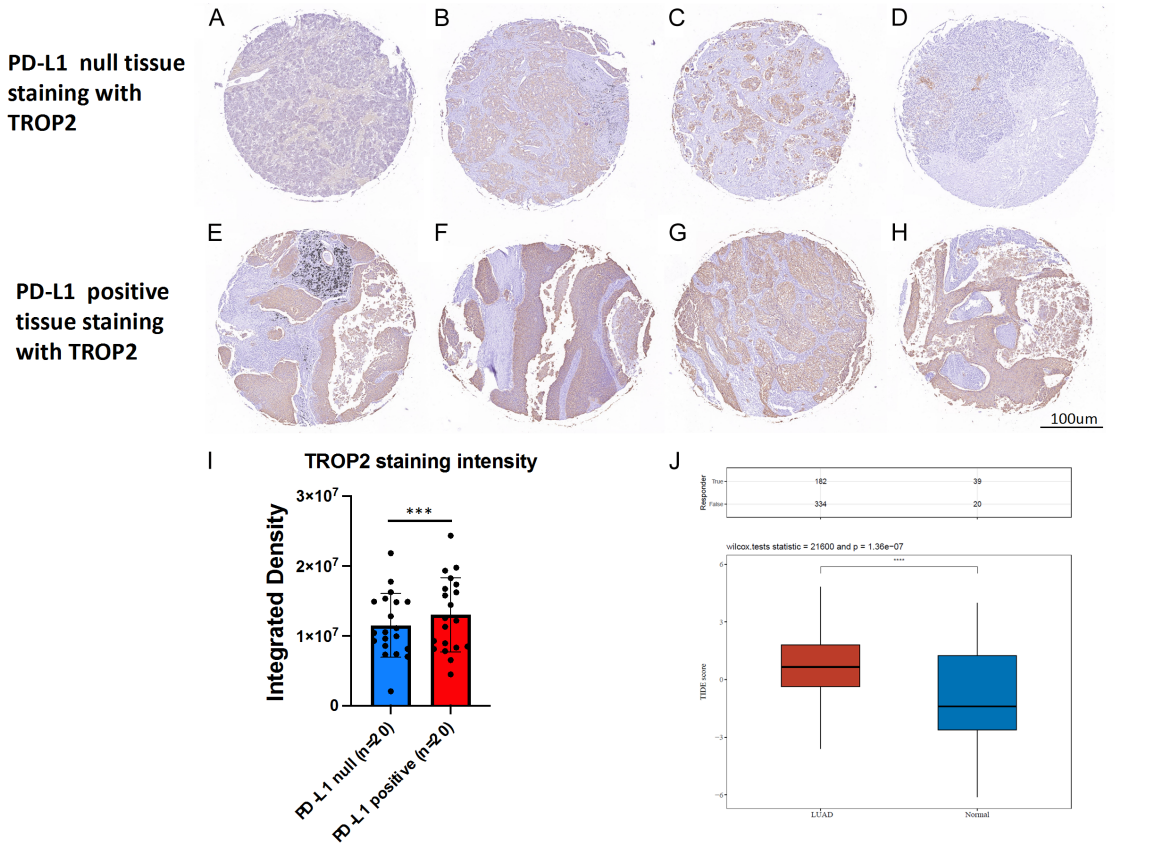

Figure 3. TROP2 expression patterns in PD-L1 null and positive lung adenocarcinoma tissues. A-D. Immunohistochemical staining of TROP2 in PD-L1 null lung adenocarcinoma samples. Four cases showing weak to moderate TROP2 staining. Scale bar = 100 μm. E-H. TROP2 staining in PD-L1 positive samples. Four cases demonstrating stronger, more widespread TROP2 expression. Scale bar = 100 μm. I. Quantitative analysis of TROP2 expression showing significantly higher integrated density in PD-L1 positive samples compared to PD-L1 null samples (***P < 0.001). J. Box plot comparing TROP2 expression in LUAD (n = 334) vs normal tissue (n = 20). Significantly higher TROP2 expression in LUAD (Wilcoxon test statistic = 21600, P = 1.36e-07). TROP2 expression is elevated in lung adenocarcinoma, with notably higher levels in PD-L1 positive tissues.

tumor microenvironment in LUAD. TROP2 signaling may directly influence chemokine production by tumor cells; based on our prior transcriptomic analysis of resistant cell lines, elevated TROP2 expression may contribute to the downregulation of key T cell-attracting chemokines. The enrichment of the MAPK pathway observed in TROP2-expressing, erlotinib-resistant cells suggests that MAPK signaling may mediate this regulation, as it is known to modulate chemokine production in epithelial cells.

Furthermore, TROP2 may promote the expression of additional immunosuppressive molecules beyond PD-L1. Our findings show higher TROP2 expression in PD-L1 positive samples, suggesting coordinated regulation. Activation of PI3K/AKT/mTOR signaling by TROP2 may further upregulate other immune checkpoint molecules, thereby creating multiple redundant immunosuppressive barriers that inhibit cytotoxic T cell function. The observed positive correlation between TROP2 expression and CAFs (Rho = 0.094, P = 3.68 × 10^{-2}) implies that TROP2 may also facilitate CAF recruitment or activation. It is hypothesized that CAFs contribute to immune evasion by establishing physical and biochemical barriers to T cell infiltration through extracellular matrix deposition and secretion of immunosuppressive cytokines. Collectively, these findings suggest that TACSTD2 selectively influences T cell infiltration patterns and stromal composition within the LUAD tumor microenvironment.

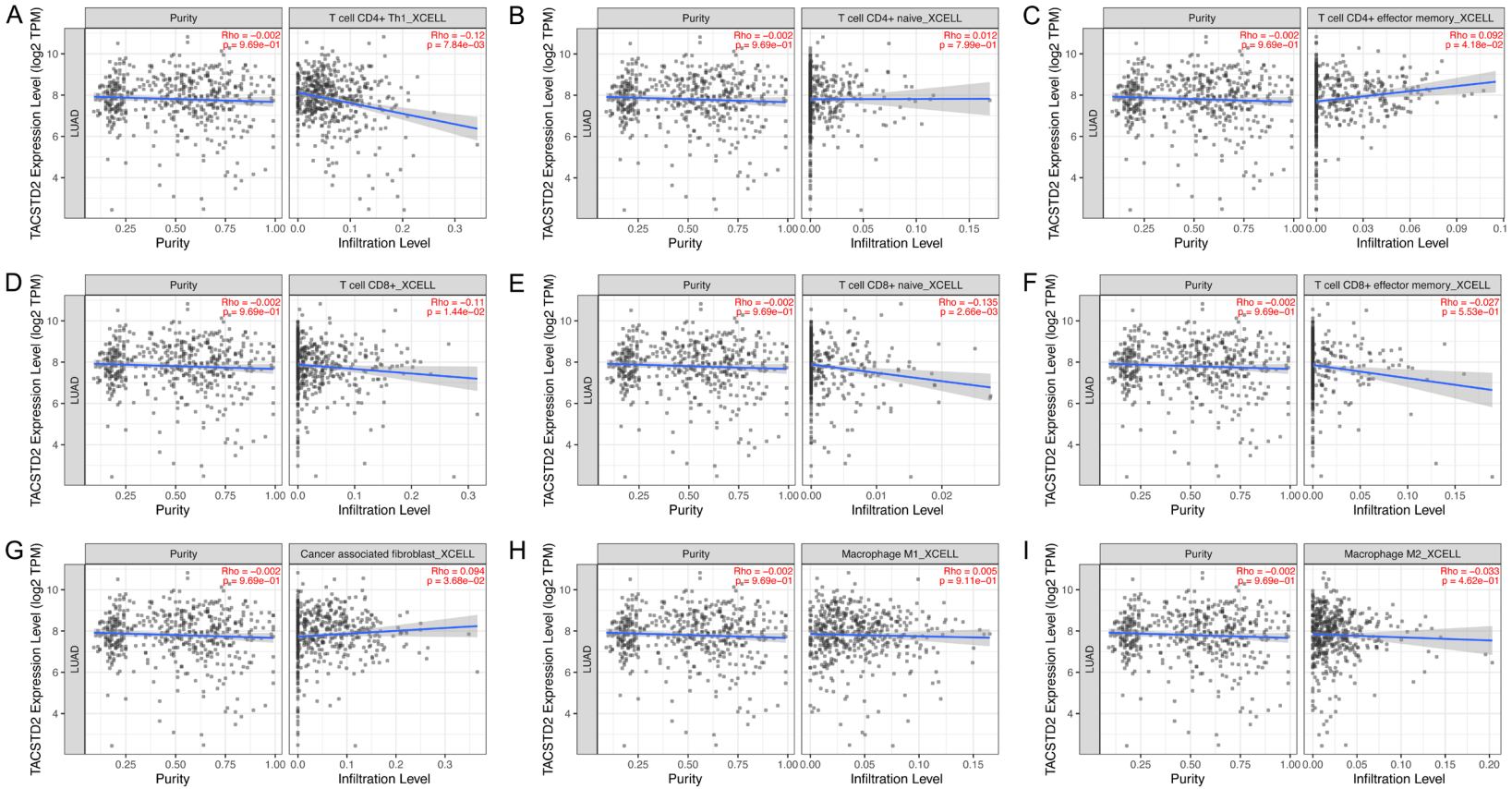

Figure 4. TACSTD2 expression correlates with distinct immune cell populations in lung adenocarcinoma. (A-I). The nine distinct plots reveal a complex landscape of correlations, with statistically significant associations emerging for specific immune cell subsets. Notably, $CD8^+$ T cells (A, Rho = -0.11, P = 1.44e-02), $CD4^+$ effector memory T cells (C, Rho = 0.092, P = 4.18e-02), $CD8^+$ naive T cells (E, Rho = -0.135, P = 2.66e-03), and cancer-associated fibroblasts (G, Rho = 0.094, P = 3.68e-02) demonstrate significant correlations with TACSTD2 expression. In contrast, other immune cell populations such as $CD4^+$ naive T cells, $CD8^+$ effector memory T cells, M1 and M2 macrophages show non-significant correlations. Each plot provides a dual perspective, examining tumor purity and immune cell infiltration, with TACSTD2 expression levels (log2 TPM) serving as the primary variable of interest, ultimately painting a nuanced picture of the molecular interplay within the tumor microenvironment.

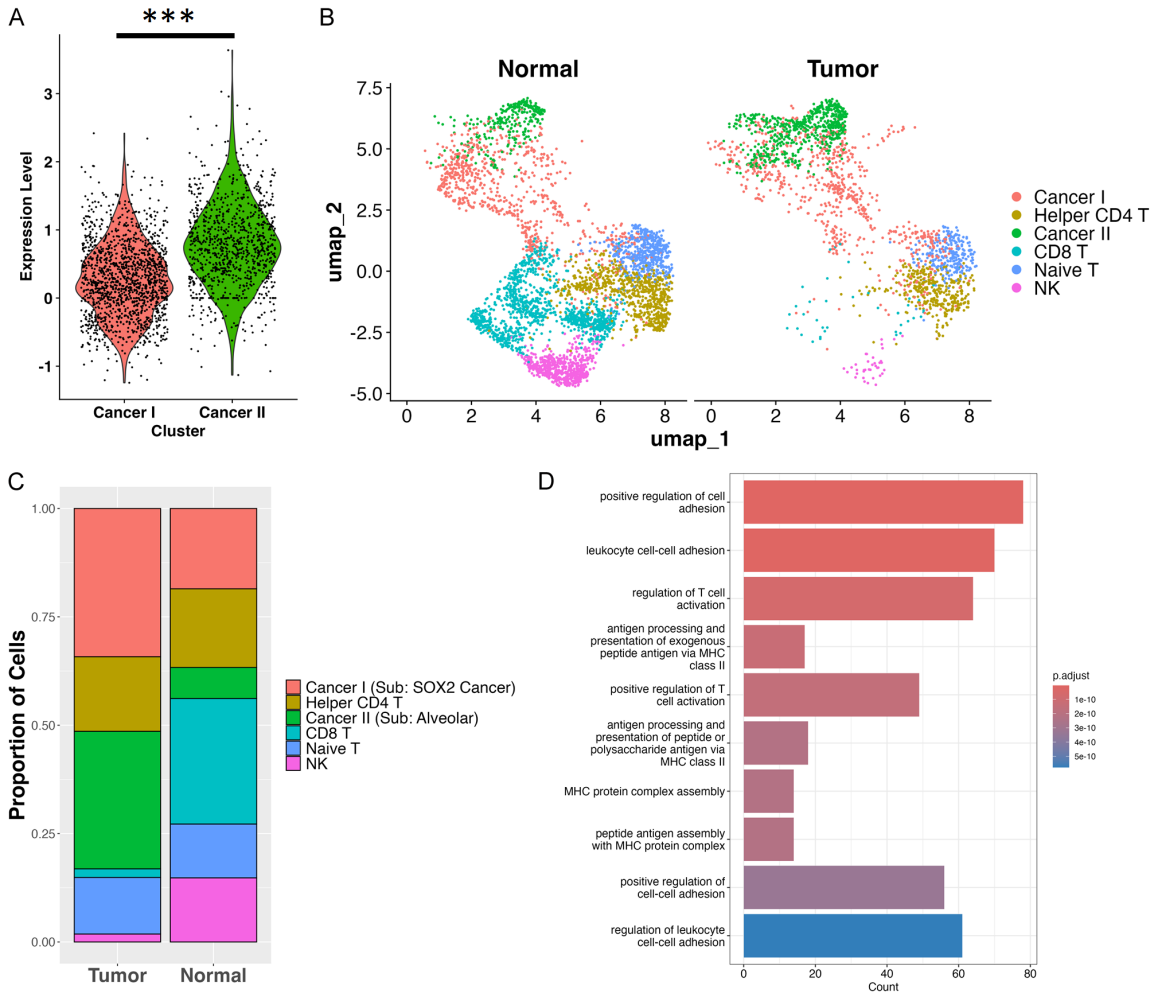

Figure 5. Single-cell analysis reveals distinct cancer subtypes and immune microenvironment alterations. A. Violin plot showing significantly higher TACSTD2 expression in Cancer II (alveolar-type) compared to Cancer I ($SOX2^+$) cells ($P < 0.001$). B. UMAP visualization comparing normal versus tumor tissues cellular landscapes, with six identified populations: Cancer I (red), Cancer II (green), Helper $CD4^+$ T cells (yellow), $CD8^+$ T cells (turquoise), Naïve T cells (blue), and NK cells (pink). C. Cellular composition analysis shows cancer cells predominate in tumor samples (~60%), while normal tissues contain higher proportions of immune cells, particularly NK cells. D. Gene ontology analysis identifies significantly enriched pathways including leukocyte cell-cell adhesion, T cell activation, and antigen processing, suggesting TACSTD2 expression may influence tumor heterogeneity and immune microenvironment composition, potentially explaining differential immunotherapy responses.

Single-cell RNA sequencing reveals distinct cancer cell populations and immune microenvironment alterations

Single-cell RNA sequencing identified two distinct cancer clusters: Cancer I ($SOX2^+$ cancer) and Cancer II (Sub-Alveolar), with significantly higher TACSTD2 expression observed in Cancer II ($P < 0.001$) (**Figure 5A**). UMAP visualization revealed differential cellular distributions between tissues, with normal samples exhibiting more distinct clustering of immune cells (**Figure 5B**). Quantitative analysis showed that cancer cells predominated in tumor samples (~60%), whereas normal tissues contained higher proportions of immune cells, particularly natural killer (NK) cells (**Figure 5C**). Gene ontology analysis further identified significant enrichment of pathways involved in leukocyte cell-cell adhesion regulation, general cell-cell adhesion, and T cell activation (**Figure 5D**). Collectively, these findings suggest that TACSTD2 expression may play a pivotal role in shaping the immune microenvironment of LUAD, particularly through its negative association with cytotoxic T cell infiltration and positive correlation

with stromal components. Moreover, the identification of two distinct cancer clusters based on TACSTD2 expression provides new insights into potential therapeutic strategies targeting specific tumor subtypes.

Taken together, this study reveals the complex interactions between TROP2 and PD-L1 in lung adenocarcinoma (LUAD), demonstrating that TACSTD2 expression significantly correlates with poor prognosis and reduced immunotherapy response (OS: HR = 1.71, P = 0.00031; PFS: HR = 2.95, P = 4.7×10^{-12}). Transcriptome analysis of drug-resistant cell lines identified alterations in steroid biosynthesis, MAPK signaling, immune receptor activity, and glycosphingolipid pathways. Immunohistochemical analysis confirmed elevated TROP2 expression in LUAD tissues (P = 1.36×10^{-7}), with higher expression levels observed in PD-L1 positive samples. Moreover, TACSTD2 expression negatively correlated with $CD8^+$ T cells (Rho = -0.11, P = 1.44×10^{-2}) and positively correlated with $CD4^+$ effector memory T cells (Rho = 0.092, P = 4.18×10^{-2}) as well as cancer-associated fibroblasts (Rho = 0.094, P = 3.68×10^{-2}). Single-cell RNA sequencing further identified two distinct cancer subtypes characterized by differential TACSTD2 expression profiles. These findings advance our understanding of the molecular mechanisms underlying TROP2 and PD-L1 interactions in LUAD, providing critical insights for the development of novel diagnostic markers and therapeutic strategies aimed at improving clinical outcomes.

Discussion

Our study reveals the complex relationship between TROP2 and PD-L1 in lung adenocarcinoma (LUAD), with implications for immunotherapy resistance and treatment development. Elevated TACSTD2 expression correlates with adverse clinical outcomes, confirming TROP2 as a negative prognostic marker in various cancers [17, 18]. Notably, high TACSTD2 expression in immunotherapy-treated patients was linked to reduced progression-free survival (HR = 2.95) and overall survival (HR = 1.71), suggesting TROP2 functions as both a prognostic indicator and predictive biomarker for immunotherapy response. Bessede et al. similarly found TROP2 associated with primary resistance to immune checkpoint inhibition in NSCLC patients [17]. This relationship likely stems from TROP2-mediated immunosuppressive effects in the tumor microenvironment, supported by our immune cell correlation analyses.

Transcriptome analysis identified distinct molecular signatures in EGFR-TKI resistant cell lines: Erlotinib-resistant cells showed MAPK signaling pathway enrichment, while Gefitinib-resistant cells exhibited immune-related pathway alterations. These findings align with Wang et al. research on abnormal NF-κB and MAPK signaling affecting osimertinib resistance and immunosuppressive tumor microenvironment formation [19]. Increased TROP2 expression links to enhanced cell proliferation, migration, and invasion in NSCLC cell lines, confirming its tumor progression role [20]. The shared 275 dysregulated genes across resistance models suggest universal EGFR-TKI resistance mechanisms. Core resistance signature analysis revealed enrichment in cell adhesion regulation, extracellular matrix organization, and transmembrane receptor signaling pathways, indicating tumor-stromal interaction and cell communication network alterations. This matches findings that acquired immune checkpoint inhibitor resistance involves complex tumor microenvironment remodeling [21, 22].

PD-L1 demonstrates notable variability as a biomarker in clinical settings, impeding effective patient stratification and treatment decisions. Ghosh et al. documented significant intra-tumor heterogeneity in PD-L1 expression along with temporal changes during disease progression and treatment response [23, 24], which helps explain inconsistent clinical responses to PD-1/PD-L1 inhibitors. PD-L1 expression is inducible by specific tumor microenvironment stimuli including inflammatory cytokines, hypoxia, and therapeutic agents. Prior research demonstrated metformin ability to modulate PD-L1 expression via the AMPK-CEBPB pathway [23], while our findings identify TROP2 signaling as an additional regulatory mechanism. This expression variability highlights the necessity for more consistent biomarkers, with our data supporting combined TROP2 and PD-L1 assessment for superior predictive accuracy. The lack of standardization in PD-L1 testing protocols including variations in antibody clones, scoring methodologies, and

positivity thresholds across clinical trials and diagnostic platforms further limits its effectiveness as a standalone biomarker. Our findings of elevated TROP2 expression specifically in PD-L1 positive samples presents a valuable complementary marker that could significantly improve patient stratification approaches.

Analysis results demonstrate TACSTD2 expression negatively correlates with cytotoxic T cells while positively correlating with $CD4^+$ effector memory T cells and cancer-associated fibroblasts, indicating TROP2 promotes immunosuppression via cytotoxic T cell reduction and immunosuppressive stromal enhancement [25]. These effects explain immunotherapy resistance in high TACSTD2 expression patients. Single-cell RNA sequencing identified distinct cancer populations with differential TACSTD2 expression - higher in alveolar-type (Cancer II) than $SOX2^+$ (Cancer I) cells. Gene ontology analysis confirmed immune interaction pathway enrichment in TACSTD2-high cells. These findings establish TROP2 as both a cancer subtype determinant and immune landscape modifier contributing to treatment resistance. TROP2 overexpression correlates with increased disease aggressiveness and reduced survival across multiple cancer types.

Our findings have important therapeutic implications. TROP2 expression could serve as a valuable biomarker for patient stratification in immunotherapy, with high TACSTD2-expressing patients potentially requiring alternative treatment approaches. The distinct resistance mechanisms we identified suggest targeted interventions - MAPK pathway inhibition for erlotinib resistance and immune pathway modulation for gefitinib resistance. The strong TROP2-PD-L1 correlation indicates potential benefits from dual-targeting strategies, with promising development of TROP2-targeted therapies like Datopotamab Deruxtecan [26] that could be combined with immune checkpoint inhibitors [27, 28]. Additionally, our identification of distinct TACSTD2-based cancer subtypes supports the development of personalized treatment approaches, particularly for patients with high-expressing Cancer II (alveolar-type) tumors who might benefit from TROP2-targeted interventions or immune microenvironment modulation. The development of TROP2-targeted antibody-drug conjugates has emerged as a promising therapeutic strategy in NSCLC.

Taken together, our study demonstrates the complex interplay between TROP2 and PD-L1 in lung adenocarcinoma, revealing significant implications for tumor progression, drug resistance, and immunotherapy response. The negative correlation between TACSTD2 expression and cytotoxic T cell infiltration, together with its positive association with immunosuppressive stromal components, provides a potential mechanistic explanation for the observed poor outcomes in high-expressing patients. These findings support the development of TROP2-targeted therapeutic strategies, either alone or in combination with immune checkpoint inhibitors, to overcome resistance and improve clinical outcomes in lung adenocarcinoma patients.

Acknowledgements

This work was supported by a grant from the National Science and Technology Council (NSTC113-2320-B-110-012, NSTC113-2314-B-037-104-MY3, and NSTC113-2314-B-037-113-MY3) and Kaohsiung Medical University (KMU 113-P36 and NYCUKMU-113-I1003).

Disclosure of conflict of interest

None.

Address correspondence to: Po-Kai Chuang, Institute of Biomedical Sciences, College of Medicine, National Sun Yat-sen University, Kaohsiung, Taiwan. Tel: 07-5252000# 7103 or 7110; E-mail: pkchuang@mail.nsysu.edu.tw

References

[1] Zhou K, Li S, Zhao Y and Cheng K. Mechanisms of drug resistance to immune checkpoint inhibitors in non-small cell lung cancer. Front Immunol 2023; 14: 1127071.

[2] Bessede A, Peyraud F, Besse B, Cousin S, Cabart M, Chomy F, Rey C, Lara O, Odin O, Nafia I, Vanhersecke L, Barlési F, Guégan JP and Italiano A. TROP2 is associated with primary resistance to immune checkpoint inhibition in patients with advanced non-small cell lung cancer. Clin Cancer Res 2024; 30: 779-785.

[3] Stanley R, Flanagan S, Reilly DO, Kearney E, Naidoo J and Dowling CM. Immunotherapy

through the lens of non-small cell lung cancer. Cancers 2023; 15: 2996.
[4] Ahmed Y, Berenguer-Pina JJ and Mahgoub T. The rise of the TROP2-targeting agents in NSCLC: new options on the horizon. Oncology 2021; 99: 673-680.
[5] Gu QZ, Nijiati A, Gao X, Tao KL, Li CD, Fan XP and Tian Z. TROP2 promotes cell proliferation and migration in osteosarcoma through PI3K/AKT signaling. Mol Med Rep 2018; 18: 1782-1788.
[6] Tang G, Tang Q, Jia L, Chen Y, Lin L, Kuai X, Gong A and Feng Z. TROP2 increases growth and metastasis of human oral squamous cell carcinoma through activation of the PI3K/Akt signaling pathway. Int J Mol Med 2019; 44: 2161-2170.
[7] Sun SY. Searching for the real function of mTOR signaling in the regulation of PD-L1 expression. Transl Oncol 2020; 13: 100847.
[8] Boussiotis VA and Patsoukis N. Effects of PD-1 signaling on immunometabolic reprogramming. Immunometabolism 2022; 4: e220007.
[9] Lu T, Li M, Zhao M, Huang Y, Bi G, Liang J, Chen Z, Zheng Y, Xi J, Lin Z, Zhan C, Jiang W, Wang Q and Tan L. Metformin inhibits human non-small cell lung cancer by regulating AMPK-CEBPB-PDL1 signaling pathway. Cancer Immunol Immunother 2022; 71: 1733-1746.
[10] Wang C, Fei K, Liu L, Duan J, Wang Z, Li S, Xu J, Zhang X, Tian Y, Qu Y, Bai H and Wang J. Abnormal activation of NF-κB and MAPK signaling pathways affect osimertinib resistance and influence the recruitment of myeloid-derived suppressor cells to shape the immunosuppressive tumor immune microenvironment. Thorac Cancer 2023; 14: 1843-1856.
[11] Denisenko TV, Budkevich IN and Zhivotovsky B. Cell death-based treatment of lung adenocarcinoma. Cell Death Dis 2018; 9: 117.
[12] Lombardi P, Filetti M, Falcone R, Altamura V, Paroni Sterbini F, Bria E, Fabi A, Giannarelli D, Scambia G and Daniele G. Overview of Trop-2 in cancer: from pre-clinical studies to future directions in clinical settings. Cancers (Basel) 2023; 15: 1744.
[13] Shvartsur A and Bonavida B. Trop2 and its overexpression in cancers: regulation and clinical/therapeutic implications. Genes Cancer 2015; 6: 84-105.
[14] Li Z, Jiang X and Zhang W. TROP2 overexpression promotes proliferation and invasion of lung adenocarcinoma cells. Biochem Biophys Res Commun 2016; 470: 197-204.
[15] Okajima D, Yasuda S, Maejima T, Karibe T, Sakurai K, Aida T, Toki T, Yamaguchi J, Kitamura M, Kamei R, Fujitani T, Honda T, Shibutani T, Muramatsu S, Nakada T, Goto R, Takahashi S, Yamaguchi M, Hamada H, Noguchi Y, Murakami M, Abe Y and Agatsuma T. Datopotamab deruxtecan, a novel TROP2-directed antibody-drug conjugate, demonstrates potent antitumor activity by efficient drug delivery to tumor cells. Mol Cancer Ther 2021; 20: 2329-2340.
[16] Qiu S, Zhang J, Wang Z, Lan H, Hou J, Zhang N, Wang X and Lu H. Targeting Trop-2 in cancer: recent research progress and clinical application. Biochim Biophys Acta Rev Cancer 2023; 1878: 188902.
[17] Khan SR, Verma S, Breadner D and Raphael J. The TROP2 paradox: enhancing precision in immunotherapy for advanced non-small cell lung cancer patients-a commentary. Transl Cancer Res 2025; 14: 660-666.
[18] Liu X, Ma L, Li J, Sun L, Yang Y, Liu T, Xing D, Yan S and Zhang M. Trop2-targeted therapies in solid tumors: advances and future directions. Theranostics 2024; 14: 3674-3692.
[19] Lee K, Kim D, Yoon S, Lee DH and Kim SW. Exploring the resistance mechanisms of second-line osimertinib and their prognostic implications using next-generation sequencing in patients with non-small-cell lung cancer. Eur J Cancer 2021; 148: 202-210.
[20] Liu X, Deng J, Yuan Y, Chen W, Sun W, Wang Y, Huang H, Liang B, Ming T, Wen J, Huang B and Xing D. Advances in Trop2-targeted therapy: Novel agents and opportunities beyond breast cancer. Pharmacol Ther 2022; 239: 108296.
[21] Khalaf K, Hana D, Chou JT, Singh C, Maćkiewicz A and Kaczmarek M. Aspects of the tumor microenvironment involved in immune resistance and drug resistance. Front Immunol 2021; 12: 656364.
[22] Ni Y, Zhou X, Yang J, Shi H, Li H, Zhao X and Ma X. The role of tumor-stroma interactions in drug resistance within tumor microenvironment. Front Cell Dev Biol 2021; 9: 637675.
[23] Ghosh C, Luong G and Sun Y. A snapshot of the PD-1/PD-L1 pathway. J Cancer 2021; 12: 2735-2746.
[24] Saito Y, Horiuchi S, Morooka H, Ibi T, Takahashi N, Ikeya T, Shimizu Y and Hoshi E. Inter-tumor heterogeneity of PD-L1 expression in non-small cell lung cancer. J Thorac Dis 2019; 11: 4982-4991.
[25] Mito R, Matsubara E, Komohara Y, Shinchi Y, Sato K, Yoshii D, Ohnishi K, Fujiwara Y, Tomita Y, Ikeda K, Sakagami T and Suzuki M. Clinical impact of TROP2 in non-small lung cancers and its correlation with abnormal p53 nuclear accumulation. Pathol Int 2020; 70: 287-294.
[26] Xiang Y, Liu X, Wang Y, Zheng D, Meng Q, Jiang L, Yang S, Zhang S, Zhang X, Liu Y and Wang B.

Mechanisms of resistance to targeted therapy and immunotherapy in non-small cell lung cancer: promising strategies to overcoming challenges. Front Immunol 2024; 15: 1366260.

[27] Zhou S and Yang H. Immunotherapy resistance in non-small-cell lung cancer: from mechanism to clinical strategies. Front Immunol 2023; 14: 1129465.

[28] Gogtay M, Aimalla N, Thirugnanasambandam RP and Ganti AK. Therapeutic potential of datopotamab deruxtecan in the treatment of advanced non-small cell lung cancer: evidence to date. Onco Targets Ther 2025; 18: 575-584.